Dynamics in the VIX complex*

Anders Merrild Posselt†

This version: May 5, 2021

* I acknowledge support from the Danish Council of Independent Research and CREATES. I am grateful for helpful comments and suggestions from Kim Christensen, Charlotte Christiansen, Thomas Kokholm and seminar participants at CREATES.

† CREATES, Department of Economics and Business Economics, Aarhus University, Fuglesangs Alle 4, 8210 Aarhus V, Denmark. Email: amp@econ.au.dk.

Dynamics in the VIX complex

Abstract

This paper provides a characterization of the dynamic interactions in the VIX complex, composed of the VIX itself, the term structure of VIX futures, and VIX ETPs. I investigate a model that summarizes the VIX futures term structure using latent factors (level, slope, and curvature) and expand it with the VIX and VIX futures demand stemming from VIX ETPs. I find evidence of VIX ETPs impacting the VIX futures term structure, but no evidence of any impacts on the VIX.

Keywords: VIX futures; Term structure analysis; VIX; VIX ETPS

JEL Classification: G13; G14

This version: May 5, 2021.

I. Introduction

In this paper, I investigate the dynamics between the term structure of VIX futures, the VIX exchange traded products (ETPs), and the VIX. I refer to the whole of these as the "VIX complex." The interactions and dynamics between the different components of the VIX complex have received much attention in financial media and by regulators (see BIS (2018)) due to fears of destabilizing feedback mechanisms. I reduce the VIX complex to a simple nonstructural VAR system of the VIX itself, VIX futures term structure factors, and hedge demand of VIX ETP issuers. Estimating the model in a state space framework, I find evidence of pricing impacts from the VIX ETPs to the VIX futures term structure on the days following a shock in hedge demand. My results contain no evidence of feedback effects from VIX ETPs or VIX futures to the VIX.

The VIX, commonly referred to as the "investor fear gauge," is probably the most used indicator of risk in the US stock market. The purpose of the index is to measure the expected volatility of the Standard and Poor's 500 index (S&P500) over the next month implied by stock index option prices. Formally, it is the square root of the risk-neutral expectation of the integrated variance of the S&P 500 over the next 30 calendar days. VIX futures were introduced in 2004 by the Chicago Board of Options Exchange (CBOE). The idea behind this innovation was to offer market participants an exposure to volatility as an asset class, with no need for delta-hedging in underlying securities. An idea that originally dates all the way back to Brenner and Galai (1989) and Whaley (1993). Furthermore, as VIX futures are exchange cleared, the counter-party risk present in variance swaps is of reduced concern. VIX futures have a variety of applications such as portfolio protection, yield enhancement, or vega-hedging by option market makers.[1]

Following a long period after the launch with poor liquidity and meager trading volume, VIX futures have become an increasingly important asset. Figure I shows a huge surge in

[1]In the options terminology, "vega" is the sensitivity of the option price to volatility.

both open interest (OI) and volume from 2009 and onward, and VIX futures are now among the most actively traded futures on the CBOE Futures Exchange (CFE). To a large extent, VIX futures have overtaken in popularity from variance swaps. Mixon and Onur (2015) document that for maturities below one year, the gross notional vega of VIX futures is more than twice as large as that of S&P 500 variance swaps. Understanding the dynamics of the VIX futures term structure is of general, vital interest, in particular to market participants applying this asset.

Figure I: VIX futures open interest and volume

Figure I shows the open interest (OI) and average daily trading volume by month for VIX futures from November 2005 to the middle of June 2020.

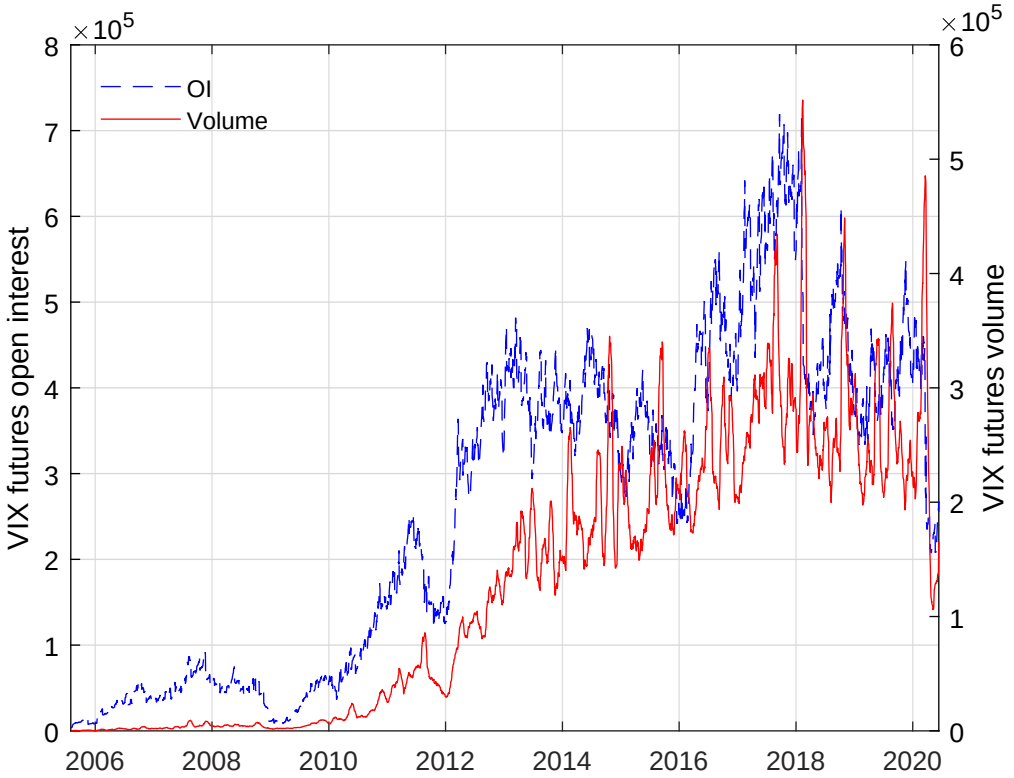

An important driver of the increased liquidity of VIX futures has been the introduction of VIX ETPs, which are structured to track the returns of a constant maturity portfolio of VIX futures (SPVXSTR). These are products that allow investors who are otherwise cut off

from derivatives, like retail investors, to obtain volatility exposure.[2] In line with the general surge in passive investing, these products have become increasingly popular. The issuers of VIX ETPs have exposure to VIX futures and will often hedge this in the same market. Consequently, the large growth in the market of VIX ETPs has raised concerns that the hedging activities of the issuers have pricing impacts that distort the VIX futures market and potentially spill over to the index options that underlie the VIX. Many market participants believe that this is exactly what occurred on February 5, 2018, referred to as "Volmagedon," where the VIX doubled, following a drop of 2.1% in the S&P500, which seems relatively small compared to the subsequent response of the VIX.[3] Also, the fixed-income and currency markets were largely unaffected, supporting the claim that this VIX spike was driven by technical, not fundamental, factors.

This paper has two main contributions. First, I illustrate how the VIX futures term structure can be fitted in a simple state space model. Second, I provide a first investigation of the dynamics of the entire VIX futures term structure, VIX ETPs, and the VIX.

The prior literature on volatility assets has studied the relation between the VIX and VIX futures. Shu and Zhang (2012) provide the earliest study on the dynamics between the VIX and VIX futures, more specifically the first- and fourth-month contracts. Relying on daily data, they detect bi-directional Granger causality (cf. Granger (1969)) between the VIX and VIX futures. However, when broken up quarter by quarter, their results indicate no information spillover from VIX futures to the VIX. Using intraday returns, Frijns et al. (2016) find weak evidence of bi-directional Granger causality between the first month contract and the VIX. Chen and Tsai (2017) also find intradaily information spillover from the first-month contract and that this increases around macro-economic announcements. Using a lead-lag measure that accounts for non-synchronous trading, Bollen et al. (2017) conduct two different analyzes using all intraday traded prices. They examine the dynamics between one of the

[2]The first two VIX ETPs, VXX and VXZ, were launched in 2009 by Barclays. Since then, other financial institutions have entered this market. Today the largest issuers are Barclays, Credit Suisse, and CitiGroup.

[3]See e.g., Bloomberg (2019).

largest VIX ETPs, VXX, and its underlying benchmark index, SPVXSTR, then between SPVXSTR and the VIX. According to their findings, lead-lag relations between the price of VXX and SPVXSTR are very short-lived, whereas SPVXSTR leads the VIX 31% of the days at the end of their sample, which spans from 2005 to 2013. By modeling the efficient VIX futures price, as an unobserved state variable, Fernandez-Perez et al. (2019) find that for the two front month VIX futures, deviations from the efficient price are more persistent after the introduction of VIX ETPs. The most recent studies are Brøgger (2020) and Todorov (2020). Brøgger (2020) finds that the rebalancing of leveraged VIX ETPs amplifies market moves in the front month VIX futures leading up to market close with no evidence of this effect being exacerbated by predatory traders. Todorov (2020) derives a synthetic VIX futures price from SPX options and VIX options, which is not influenced by hedging activity of ETP issuers, thereby obtaining a fundamental value of the VIX futures. For the two front month VIX futures, the difference between the fundamental and the observed value is strongly related to hedge demand of ETP issuers.

To the best of my knowledge, all previous studies of the subject consider only the front month VIX futures and not the entire term structure. In this study, I explore the dynamics of the entire VIX futures term structure, together with the VIX and VIX ETPs. The majority of VIX ETPs are exposed to the front-month VIX futures, but pricing impacts in these may potentially spill over to the entire curve. For instance, following a large shock in the short-dated contracts, a market participant with exposure to both the short and long end is likely to alter her position held in the long dated contracts, to keep exposure fixed.[4] As the liquidity of VIX futures tend to be decreasing in time-to-maturity, the price distortions may be most persistent at the long end of the curve.

Potential feedback effects have been investigated in other markets as well. The evidence of stock ETPs impacting the underlying stocks (see Cheng and Madhavan (2009), Schum et al. (2016), Ivanov and Lenkey (2018), and Ben-David et al. (2018)) is rather mixed, and

[4]E.g. A market participant may partially finance a long volatility exposure in the short dated VIX futures, by selling the longer dated VIX futures.

the magnitude tend to be small because, unlike VIX ETPs, they comprise a small fraction of the market for the underling asset. Investigating the options market, the studies by Ni et al. (2005), Golez and Jackwerth (2012), and Ni et al. (2021) find that delta-hedging by dealers, has an economically significant impact on the price of the underlying stocks.

The analysis of this paper is two-fold and follows the structure of Diebold et al. (2006). First, I apply the Dynamic Nelson-Siegel (DNS) model of Diebold and Li (2006) to fit the VIX futures term structure. The DNS model provides a nice dimensionality reduction of the term structure, which facilitates the analysis of the term structure dynamics. The three factors of the DNS model, level, slope, and curvature, are estimated as latent state variables in a state space model as in Diebold et al. (2006) and Koopman et al. (2010). The estimated model fits the term structure very well and has very low pricing errors, something which can be difficult to obtain for many dynamic derivative valuation models (cf. Menacía and Sentana (2013)). Next, I expand the state space model, with the VIX and an estimate of VIX futures hedge demand from VIX ETP issuers. Thus, the VIX complex is modeled as a nonstructural VAR(1) system, whereby I can provide a characterization of the dynamics between the different components. I find that a shock to the demand variable impacts the curvature factor, suggesting that the hedge rebalancing of VIX ETP distorts the VIX futures term structure. I find no evidence of an impact from hedge demand to the VIX. Finally, my results suggest that demand reverses quickly following a spike in the VIX, in line with the findings of Nielsen and Posselt (2020).

The paper is organized into three additional sections. In Section II, I describe and estimate the basic VIX futures-only model - that is, the model of just VIX futures without the other components of the VIX complex. In Section III, I incorporate the VIX and hedge demand into the model. Section IV provides a conclusion.

II. The VIX futures-only model

In this section, I introduce a factor model of the VIX futures term structure without the additional components of the entire VIX complex (the VIX and VIX ETPs). The purpose of this is, first of all, to introduce the state space framework that I use throughout the paper. Furthermore, this VIX futures-only model will serve as a useful benchmark to which I can subsequently compare the full model that incorporates the remaining components of the VIX complex. But first, I provide a brief description of VIX futures.

II.A. Briefly about VIX futures

The financial assets of interest in this study are VIX futures. These trade on the CBOE Futures Exchange (CFE), they are cash-settled with a contract multiplier of $1000 and have both weekly and monthly expiration, usually on Wednesday mornings. As indicated by the name, the underlying index of these futures is the VIX. CBOE maintains a formal real-time calculation of the VIX. However, the exercise-settlement value of VIX futures is calculated using the auction clearing prices of SPX options in an auction called the Special Opening Quotation (SOQ).[5] At any given point in time, there are several futures contracts trading, each with a different time to maturity. VX1 is the ticker of the monthly futures contract with the shortest time to maturity, VX2 for the second shortest, and so on. For example, at the time of this writing, VX1 expires on August 18, 2020, and VX2 expires on September 15, 2020. Thus at any point in time, there is an entire term structure of VIX futures available. The liquidity is mainly concentrated in the two nearest-to-maturity contracts, VX1 and VX2, and is in general best in the monthly contracts.

[5] See, e.g., Griffin and Shams (2018) for more on the settlement details.

II.B. The Dynamic Nelson-Siegel model

Following the work of Nelson and Siegel (1987), Diebold and Li (2006) introduce the Dynamic Nelson-Siegel (DNS) model to fit a set of yields, $y_t(\tau_i)$, of N different maturities, $\tau_1 < \cdots < \tau_N$, available at time $t = 1,...,T$ using the three factor model:

$$y_t(\tau_i) = \beta_{1t} + \beta_{2t}\left(\frac{1 - e^{-\lambda\tau_i}}{\lambda\tau_i}\right) + \beta_{3t}\left(\frac{1 - e^{-\lambda\tau_i}}{\lambda\tau_i} - e^{-\lambda\tau_i}\right) + \varepsilon_{it}, \tag{1}$$

with the disturbances, $\varepsilon_{1t}, ..., \varepsilon_{Nt}$, assumed to be independent with mean zero and constant variance σ_t^2 for a given time t.

β_{1t}, β_{2t}, and β_{3t} can be interpreted as latent dynamic factors. β_{1t} is a long-term factor since $\lim_{\tau\to\infty} y_t(\tau_i) = \beta_{1t}$. It is labeled "Level" since the loading on this factor is identical at all maturities, and thereby it controls the level of the entire yield curve. The loading on β_{2t}, $(1\text{-}e^{-\lambda\tau_i})/(\lambda\tau_i)$, is a function that starts at one and decays monotonically and quickly to 0, implying that this is a short-term factor. The short end of the curve is given as, $\lim_{\tau\downarrow 0} y_t(\tau_i) = \beta_{1t} + \beta_{2t}$, and defining the slope of the yield curve as $y_t(\infty) - y_t(0)$, then this is exactly equal to $-\beta_{2t}$. Thus this factor is denoted "Slope." Finally, the loading on β_{3t}, $(1\text{-}e^{-\lambda\tau_i})/(\lambda\tau_i)\text{-}e^{-\lambda\tau_i}$, is a function starting at 0, which increases and then decays to 0 for longer maturities, hence we may view this as a medium term factor. It loads minimally on the short and long end of the curve but impacts the medium terms. Thus this factor is denoted "Curvature." The last parameter in the DNS model, λ, controls the exponentially decaying rate of the loadings for the slope and curvature factors, and a smaller value produces a slower decay. Figure II presents a plot of the three different factor loadings with $\lambda = 0.018$, as an example.

In the original Nelson and Siegel (1987) model λ is time-varying, so at every time point t, the parameters of the model would be estimated by nonlinear least squares. However, in the DNS model of Diebold and Li (2006), λ is fixed at a prespecified value, which facilitates the use of ordinary least squares to estimate the betas (factors).

Figure II: Factor loadings

Figure II plots the factor loadings in the three-factor Nelson-Siegel model. I fix $\lambda_t = 0.018$.

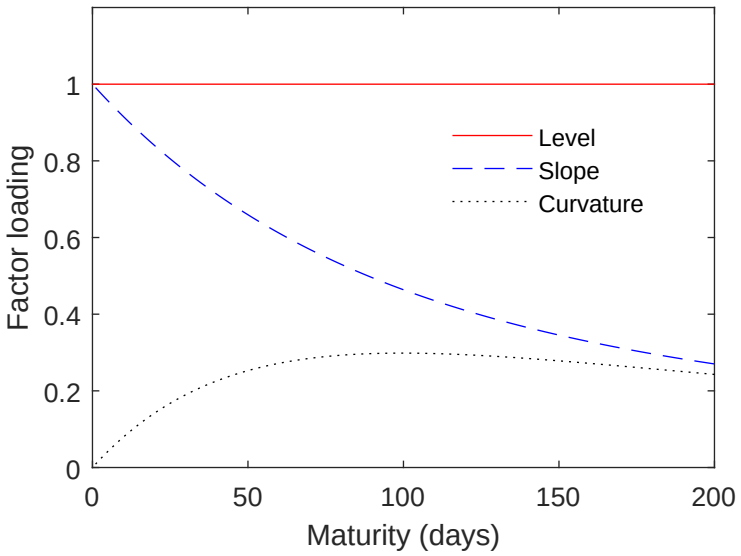

The DNS is a purely statistical model that neither relies on no-arbitrage nor equilibrium assumptions, so, despite the original purpose of yield-curve fitting, there are no theoretical arguments against applying it to other asset classes. Previous studies have found it quite useful in the context of derivative prices. For instance, Grønborg and Lunde (2016) use it to fit the term structure of oil futures, and West (2012) uses it in the setting of futures on various agricultural products. More related to my study are Guo et al. (2014), Guo et al. (2017), and Chen et al. (2018), who all fit the term structure of option-implied volatilities, for a fixed strike price, by means of the DNS.

In my setting, $y_t(\tau_i)$ denotes the VIX futures price with maturity τ_i (measured as days to maturity) at time, t.

II.C. State space representation of the Dynamic Nelson-Siegel model

I apply the same methodology as in Diebold et al. (2006) and Koopman et al. (2010) but in the setting of VIX futures prices instead of interest rates. I estimate the time series of the latent factors in the DNS model (Level, Slope, and Curvature) via a state space model. In

this setting, Equation (1) is rewritten as:

$$\mathbf{y}_t = \mathbf{\Lambda}(\lambda)\boldsymbol{\beta}_t + \boldsymbol{\varepsilon}_t, \qquad \boldsymbol{\varepsilon}_t \sim \text{NID}(0, \mathbf{R}), t = 1, ..., T, \tag{2}$$

with observation vector $\mathbf{y}_t = (y_t(\tau_1), ..., y_t(\tau_N))'$ (where $y_t(\tau_i)$ is the VIX futures price with maturity τ_i), disturbance vector $\varepsilon_t = (\varepsilon_{1t}, ...\varepsilon_{Nt})$', and an $N\times$ 3 factor loading matrix $\mathbf{\Lambda}(\lambda)$, where the i-th row is given by:

$$\mathbf{\Lambda}_i(\lambda) = \left(1, \left(\frac{1 - e^{-\lambda\tau_i}}{\lambda\tau_i}\right), \left(\frac{1 - e^{-\lambda\tau_i}}{\lambda\tau_i} - e^{-\lambda\tau_i}\right)\right). \tag{3}$$

Then, let $\boldsymbol{\beta}_t = (\text{Level}_t, \text{Slope}_t, \text{Curvature}_t)'$ denote the latent state vector, and the time series processes for the latent factors are modeled by the vector autoregressive (VAR) process:

$$\boldsymbol{\beta}_{t+1} = (\mathbf{I} - \mathbf{\Phi})\boldsymbol{\mu} + \mathbf{\Phi}\boldsymbol{\beta}_t + \boldsymbol{\eta}_t, \qquad \boldsymbol{\eta}_t \sim \text{NID}(0, \mathbf{Q}), \tag{4}$$

for t = 1,...,T, with mean vector $\boldsymbol{\mu}$, coefficient matrix $\mathbf{\Phi}$, and variance matrix $\mathbf{Q}$.

In my entire analysis, I will assume that the matrix $\mathbf{Q}$ is non-diagonal, and the matrix $\mathbf{R}$ is diagonal. The latter assumption implies that the deviations of the futures prices at various maturities from the fitted prices are uncorrelated. This assumption is quite common in the yield curve literature but is also applied in previous studies of VIX futures-pricing, see Menacía and Sentana (2013). The assumption of an unrestricted $\mathbf{Q}$ matrix allows the shocks to the three term structure factors to be correlated.

II.D. Data

I examine VIX futures, with monthly expiration, on a sample running from September 2011 to the middle of June 2020. I consider the 1st, 2nd, 3rd, 4th, 5th, 6th, 7th, and 8th contract, which over my sample has an average time to maturity of 16, 46, 77, 107, 137, 168, 199, and 229 days respectively. Occasionally there is a 9th and 10th contract available, but I

disregard these due to their inconsistent availability. I use the end-of-day closing prices collected from CBOE. In Figure III, I provide a three-dimensional plot of my VIX futures term structure data. For the main part of the sample period, the shape is upward sloping (contango). However, a sharp downward slope (backwardation) is very pronounced at the end of the sample during the large Covid19 stock market selloff and also at the 2018 Volmagedon event, where the VIX complex blew up. Regarding the level of the entire term structure, we also detect a temporal variation. At the beginning of the sample, it is rather elevated. Then it decreases steadily to a lower plateau at which it remains (occasionally lifted) for the major part of the sample period, reflecting the tenacious run-up in stocks of the past decade. At the very end of the sample, it jumps to a historical high, caused by the Covid19 market turmoil.

Figure III: Cross section of VIX futures

Figure III depicts the cross section of VIX futures during my sample, spanning from September 2011 to the middle of June 2020. I consider the 1st to the 8th (included) contract. The VIX futures have an average time to maturity ranging from 16 days to 229 days.

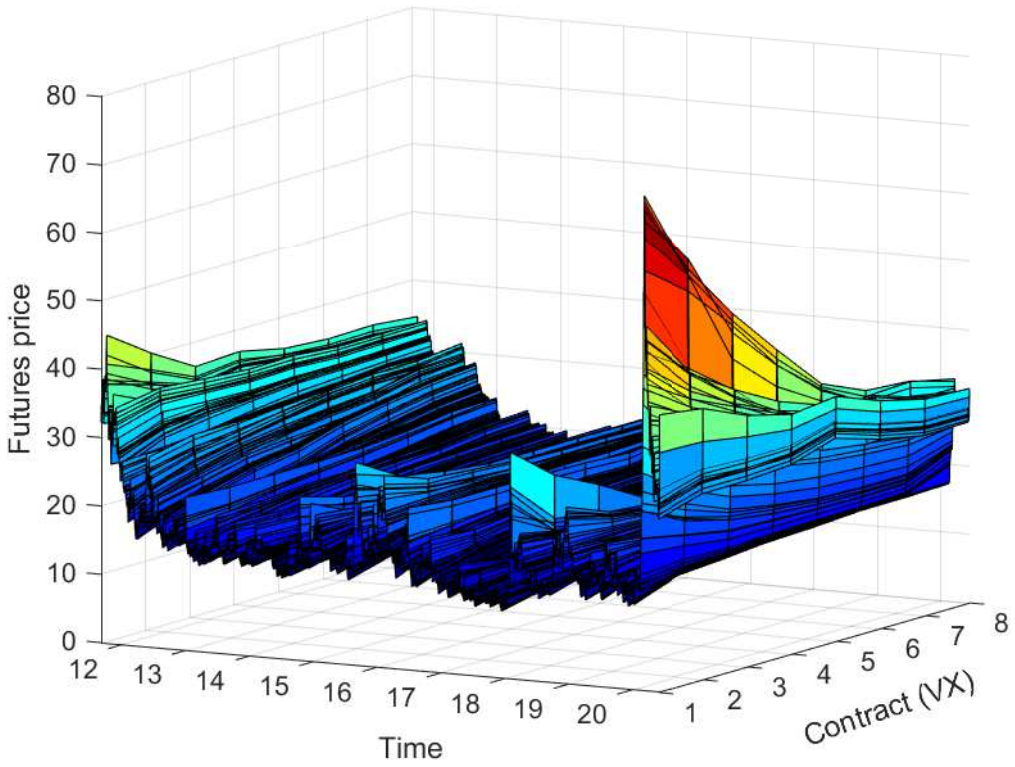

Descriptive statistics of the eight contracts are provided in Table I. The typical contango of the term structure is clearly reflected in the mean prices (column 2), as these are monotonically increasing in maturity. The column with max prices depicts the typical backwardation of the term structure when stock-market volatility is high. Furthermore, we see that the volatility of the futures prices is highest for the short end, monotonically decreasing for longer maturities, reflecting the typical the mean reverting nature of the VIX (cf. Whaley (2009)). OI and volume is monotonically decreasing in maturity, reflecting that liquidity is mainly concentrated at the front of the term structure.

Table I: Descriptive statistics, VIX futures

This table reports descriptive statistics of the VIX futures considered in this study. Column 2 - 4 reports the mean, standard deviation, min, and max, respectively, of the prices. Column 6 and 7 reports the average OI and volume respectively.

Futures contract	Mean	Std. dev.	Min.	Max.	OI	Volume
VX1	17.38	6.31	9.88	72.63	133,609	90,995
VX2	18.13	5.41	11.33	61.43	131,582	76,277
VX3	18.67	4.82	12.23	51.5	46,619	23,197
VX4	19.09	4.47	12.98	44.30	32,781	11,500
VX5	19.50	4.34	13.48	37.48	26,504	6,807
VX6	19.85	4.24	13.93	35.15	19,510	4,102
VX7	20.15	4.14	14.53	35.30	10,882	2,396
VX8	20.39	4.02	14.90	34.65	3,681	681

II.E. Fitting the VIX futures term structure

As discussed above, the VIX futures-only model forms a state space system, with a VAR(1) state equation summarizing the dynamics of the vector of latent state variables and a linear measurement equation relating the observed futures to the state vector. The parameters in the VAR coefficient matrix $\mathbf{\Phi}$, the variance matrices $\mathbf{R}$ and $\mathbf{Q}$, the mean vector $\boldsymbol{\mu}$, and λ are treated as unknown coefficients to be estimated. They are all estimated using maximum likelihood estimation. That is, for a given parameter configuration, I use the Kalman filter to compute optimal VIX futures predictions and the corresponding prediction errors (see Appendix A), after which I evaluate the Gaussian likelihood function using the prediction-error

decomposition of the likelihood. For maximizing the likelihood, I use a numerical method. Specifically, I deploy the Covariance Matrix Adaptation Evolution Strategy (CMA-ES), see Hansen and Ostermeier (1996).[6]

In the first panel of Table II, I present the estimation results for $\mathbf{\Phi}$.[7] These results indicate highly persistent dynamics for all three factors, with estimated own-lag coefficients of 0.98, 0.97, and 0.95 for Level_t, Slope_t, and Curvature_t respectively. The cross-factor dynamics all appear to be of minor importance (-0.01 and 0.01 for Level_t, -0.01 and -0.04 for Slope_t, and 0.03 and 0.06 for Curvature_t) although all except for two are statistically significant at the 1% level. The estimates also indicate that persistence decreases (measured by the diagonal elements of $\mathbf{\Phi}$), and transition shock volatility increases (measured by the diagonal elements of $\mathbf{Q}$), as we move from Level_t to Slope_t to Curvature_t. Interestingly, these findings are in line with the factor dynamics of the yield curve in Diebold et al. (2006). If we consider the remaining estimates, they all appear sensible; the mean level factor is 25.5, which is quite close to the mean price of the 8th VIX futures contract. The mean slope factor is approximately -6.40, which indicates that the term structure on average is in contango, and the mean curvature factor is -3.73.[8] In Panel B, I report the upper diagonal of the estimated $\mathbf{Q}$ matrix, and we see that all the off-diagonal elements are significantly different from zero. Finally, I obtain an estimate of λ of 0.0181, which implies that the loading on the curvature factor is maximized at a maturity of 98 days.

The VIX futures-only model fits the term structure very well, also in comparison with models applied in previous studies (see Menacía and Sentana (2013) for a comparison of different dynamic models). Table III contains the mean and standard deviation of the measurement errors for each of the eight VIX futures that I consider. The error is the lowest for VX7 (0.01). However, it is negligible across all the contracts. The standard deviation also appears quite low-ranging, from 0.17 (VX1) to 0.25 (VX6) and a mean of 0.21 across all

[6]MATLAB implementation is made publicly available by Nikolaus Hansen.

[7]Stationarity is assured since all eigenvalues are below 1.

[8]Recall from Section II.B that slope is defined as short end minus long end, so that a negative mean slope implies that the VIX futures price tend to increase in maturity.

Table II: Parameter estimates of the VIX futures-only model

Table II reports the estimates of the parameter coefficients of the state space model. Panel A reports the VAR coefficient matrix $\boldsymbol{\Phi}$ and the mean vector $\boldsymbol{\mu}$. Panel B reports the coefficients of the variance matrix $\boldsymbol{Q}$. Standard errors are given in parenthesis. ** represents significance at 1%.

Panel A: Estimates of Φ matrix and μ vector				
	Level_{t-1}	Slope_{t-1}	Curvature_{t-1}	μ
Level_t	0.98**	-0.01**	0.01	25.51**
	(0.00)	(0.00)	(0.01)	(1.47)
Slope_t	-0.01	0.97**	-0.04**	-6.36**
	(0.01)	(0.00)	(0.02)	(0.80)
Curvature_t	0.03**	0.06**	0.95**	-3.73**
	(0.01)	(0.02)	(0.03)	(0.66)

Panel B: Estimate of Q matrix			
	Level_t	Slope_t	Curvature_t
Level_t	0.72**	-0.10**	-0.89**
	(0.04)	(0.03)	(0.07)
Slope_t		2.65**	-0.17**
		(0.03)	(0.04)
Curvature_t			2.77**
			(0.12)

contracts.

Table III: Summary statistics of measurement errors - futures-only model

Futures contract	Mean	Standard deviation
VX1	-0.04	0.17
VX2	0.06	0.24
VX3	0.03	0.19
VX4	-0.04	0.18
VX5	-0.03	0.24
VX6	-0.02	0.25
VX7	0.01	0.18
VX8	0.02	0.21

In Figure IV, I provide plots of the raw term structure together with the 3-factor fitted curve for selected dates. From this, the three-factor model is obviously capable of replicating the VIX futures term structure for a variety of shapes: upward sloping, downward sloping, humped and inverted humped. It does, however, have difficulties at dates with large dispersion in the futures prices, and several minima or maxima, visible in Panel (b) and Panel (d). It is

quite likely that large dispersion arises due to liquidity effects. However, in the case of Panel (d), the spike in VX5 is likely due to the market pricing of increased uncertainty and market volatility around the 2020 US-election.

Now finally, for this section, let us consider the time series of the filtered latent term structure factors. In Figure V, I provide a plot of these together with the respective empirical proxies. Panel (a), depicts the level factor along with the price of VX8. Indeed these series seem very related, and the correlation between the two is 0.89. The level is rather elevated at the beginning of the sample but declines steadily until it appears persistently low from 2013, interrupted by brief spikes reflecting short periods of market turmoil. Then in the final part of the sample, it increases significantly during the Covid19 market turmoil. Turning to the slope factor, depicted in Panel (b), we see that this factor is also very closely related to its empirical proxy, the price of VX8 minus the price of VX1. The correlation between the slope factor and VX8 minus VX1 is -0.99. Throughout the sample period, the slope factor is rather persistent at a negative level implying an upward-sloping term structure (contango). However, we note several sharp spikes to positive levels, which inverts the term structure. These are very pronounced end-of-August 2015 (devaluation of the Renminbi), beginning of February 2018 (Volmagedon), and end-of-March 2020 (Covid19), which are all periods with increased volatility in financial markets. For the curvature factor, Panel (c) reveals a very close relation with the empirical proxy ($2 \times$ VX3-(VX1+VX8)), confirmed by a correlation of 0.92, which again lends credibility to the interpretation of this factor. We note the downward spikes almost simultaneously with the downward spikes in the slope factor, at high-volatility periods.

III. A model of the VIX complex

Given the ability of the level, slope and curvature factors to provide a good representation of the VIX futures term structure, it is of interest to relate these to the two other components of the VIX complex, which are the VIX itself and VIX ETPs. I do this in the following

Figure IV: Selected fitted (model-based) term structures of VIX futures

Figure IV shows the fitted term structure of VIX futures for selected dates, together with the actual futures prices.

(a) Term structure on 01/06/2012

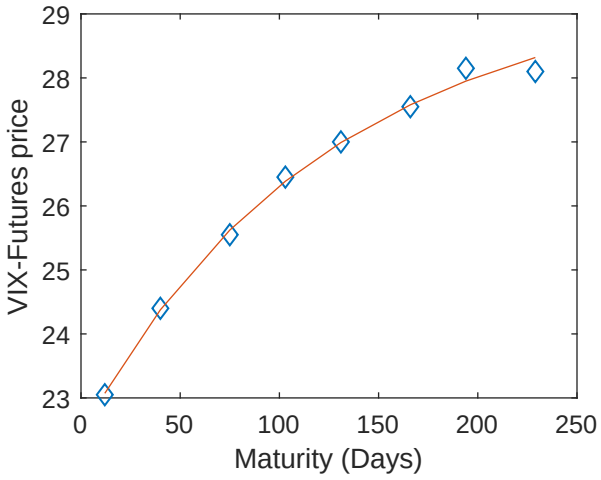

(b) Term structure on 01/28/2019

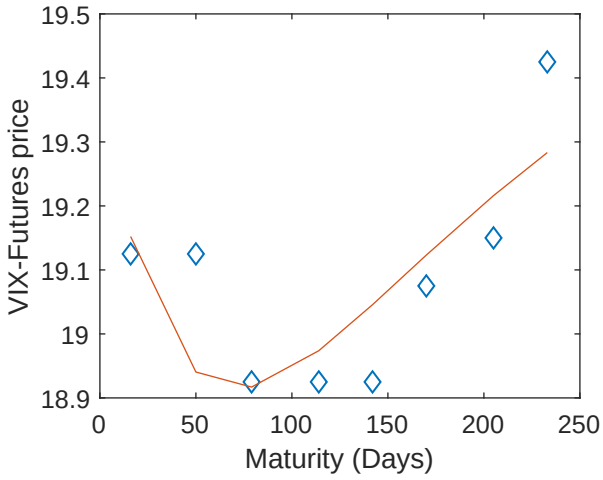

(c) Term structure on 03/17/2020

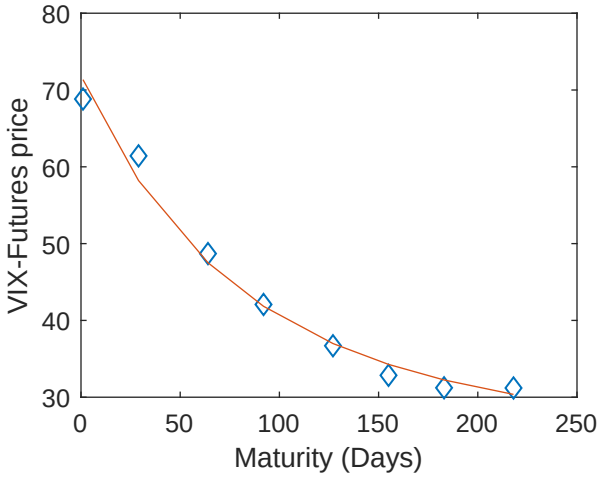

(d) Term structure on 05/27/2020

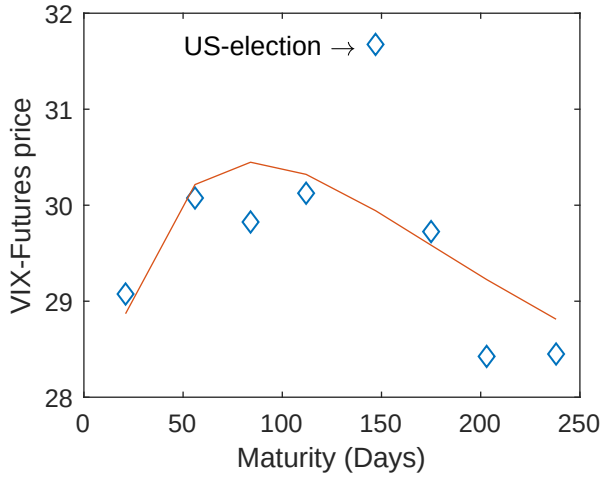

Figure V: Latent factors

Figure V shows the time series of the filtered latent term structure factors, together with the empirical proxies. Correlations are; 0.89 for Level and VX8, -0.99 for Slope and VX8 minus VX1, and 0.92 for Curvature and 2×VX3-(VX1+VX8).

(a) Level

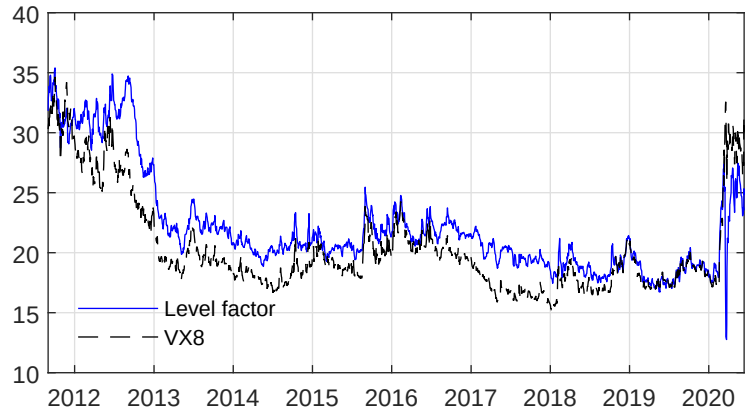

(b) Slope

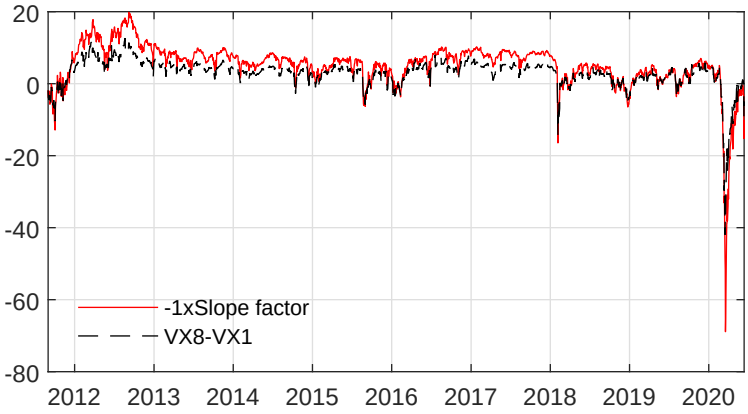

(c) Curvature

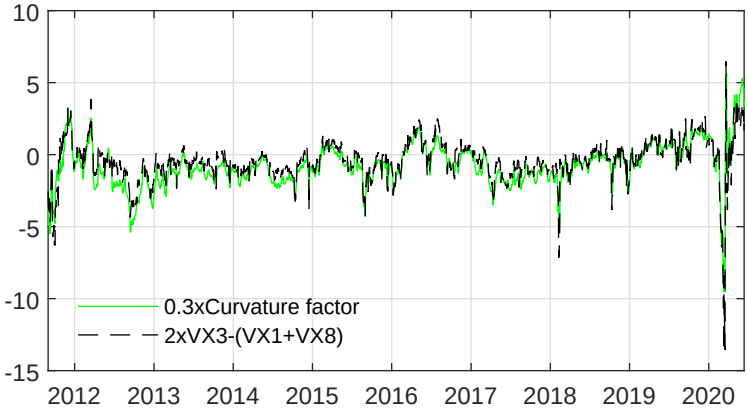

subsections by expanding the above state space model. However, I first elaborate on the introduction of the VIX ETPs and explain the potential feedback mechanism that these products may have induced in the VIX complex. Then, I estimate the expanded state space model and analyze the dynamic interactions between the VIX futures term structure, the VIX, and the VIX ETPs, obtaining a characterization of the VIX complex as a whole.

III.A. VIX ETPs

ETPs based on VIX futures were introduced in 2009. Since then, they have increased tremendously in popularity and are today among the most liquid and popular products in all of the ETP space. They all track the returns of a portfolio with a constant maturity in VIX futures, however, with variations in the maturity, leverage, and direction of exposure (as some products have an inverse exposure).[9] Panel (a), in Figure VI, shows the development in total assets under management (AUM) of the VIX ETPs split on the type of product, i.e., unleveraged, leveraged, and inverse. We see that the size of the overall product group has grown appreciably since the inception of the first product and reaches a peak of about $11 bn. during the Covid19 stock market crash in the spring of 2020. During the first years after the introduction, normal products (i.e., direct, unleveraged exposure) constitute the entire market. But from 2012, inverse products make up a larger and larger share of the market, peaking at approximately 65% in February 2018. The effects of the Volmagedon event on February 5, 2018, then make a dramatic reduction in the AUM of inverse products, clearly visible in the figure. The used-to-be largest inverse product, XIV, lost over 90% of net-asset-value during this event and was subsequently closed by the issuer. From 2016 we see that leveraged products make up an increasingly larger share of the market, and by the end of my sample, it is the largest group with a total AUM of $1.5 bn. Panel (b) depicts the AUM split by the target maturity of the strategy that the products track. This maturity is

[9]The benchmark that most ETPs track is SPVXSTR. Formally this is an index maintained by Standard & Poor's that tracks the returns of a portfolio that rolls daily between the two front-month VIX futures contracts in order to maintain a constant maturity of 30 days. SPXMTR is similar only it tracks the fourth-, fifth-, sixth-, and seven-month futures to maintain a constant average maturity of five 150 days.

either 30 days (short-term) or 150 days (mid-term). It is quite clear that throughout the sample, short-term products are by far the largest group.

Figure VI: VIX ETP assets under management

Figure VI shows the asset under management of VIX ETPs grouped by leverage (Panel (a)) and by maturity (Panel (b)) from January 2020 through the middle of June 2020.

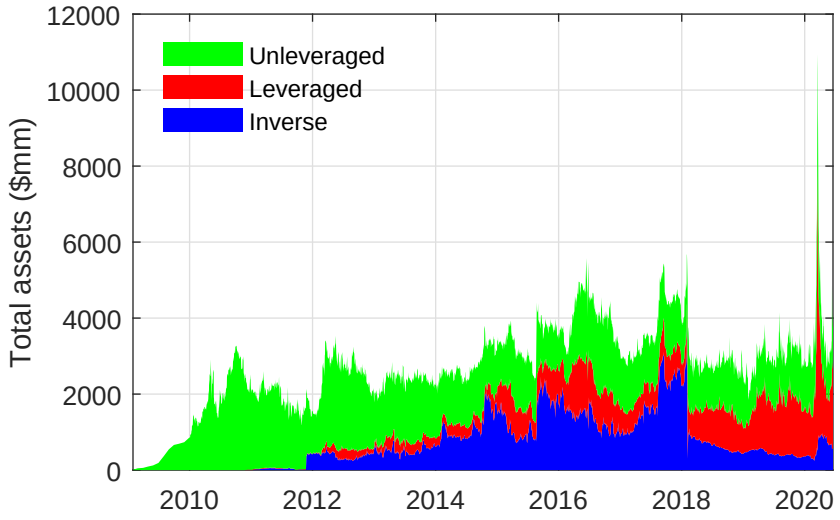

(a) AUM split by leverage

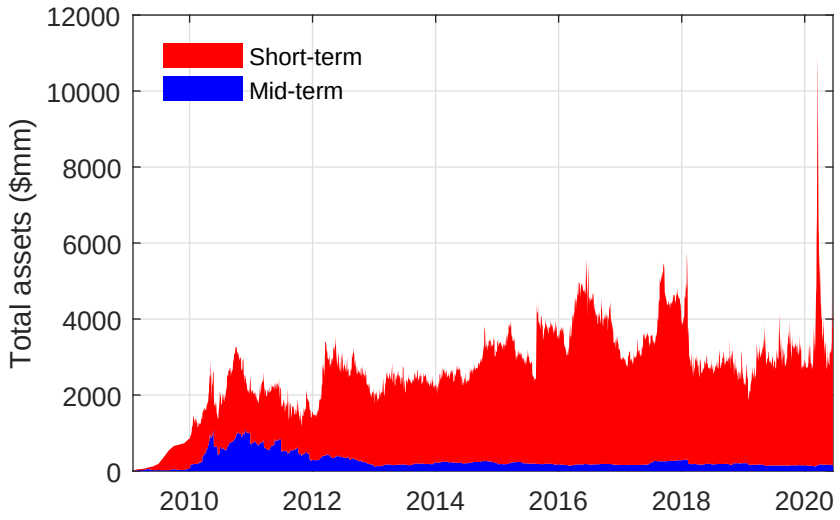

(b) AUM split by maturity

As VIX futures are the underlying assets of a VIX ETP, the issuer of the ETP is exposed to changes in the VIX futures prices. Consequently, there will be a hedging demand from the

issuers entering the VIX futures market. Todorov (2020) shows that the hedging demand, in dollar terms, of an ETP for the first-month contract, VX1, can be estimated as:

$$D^{\$}_{t,VX1} = \underbrace{-\frac{L}{K}A_{t-1}(1+Lr_t)}_{\text{calendar reb.}} + \underbrace{\alpha_{t-1}A_{t-1}L(L-1)r_t}_{\text{leverage reb.}} + \underbrace{(\alpha_{t-1}-\frac{1}{K})Lu_t}_{\text{flow reb.}} + \underbrace{\alpha_{t-1}(1-\beta_{t-1})A_{t-1}L(r_t^{VX2}-r_t^{VX1})}_{\text{remainder}}. \quad (5)$$

Many different variables enter this expression, which require a description; L denotes the leverage target of the ETP (L<0 for an inverse product and L=1 for a non-leveraged product), A_{t-1} is the AUM at time $t-1$, u_t is the capital flow (inflows (outflows) when customers buy (sell)) at time t, and K is the target maturity of the ETP. Let T_1 and T_2 denote the time to maturity of the first- and second-month futures contracts, respectively. Then in order to have a 30 days average maturity of the entire position in VIX futures, a fraction, α_{t-1}, must be invested in the first-month contract such that $\alpha_{t-1}T_1+(1-\alpha_{t-1})T_2 = 30\,\text{days}$. r_t^{VX1} and r_t^{VX2} are the net returns on the first-month and the second-month futures contracts, respectively. $\beta_{t-1} = \frac{\alpha_{t-1}\text{VX1}_{t-1}}{\alpha_{t-1}\text{VX1}_{t-1}+(1-\alpha_{t-1})\text{VX2}_{t-1}}$ where VX1_{t-1} and VX2_{t-1} are the futures prices at $t-1$. $r_t = \beta_{t-1}r_t^{VX1} + (1-\beta_{t-1})r_t^{VX2}$ is the net return on the benchmark index. Analogously, the total dollar hedge demand for the second-month futures contract, VX2, is estimated as:

$$D^{\$}_{t,VX2} = \underbrace{\frac{L}{K}A_{t-1}(1+Lr_t)}_{\text{calendar reb.}} + \underbrace{(1-\alpha_{t-1})A_{t-1}L(L-1)r_t}_{\text{leverage reb.}} + \underbrace{(1-\alpha_{t-1}-\frac{1}{K})Lu_t}_{\text{flow reb.}} + \underbrace{\beta_{t-1}(1-\alpha_{t-1})A_{t-1}L(r_t^{VX2}-r_t^{VX1})}_{\text{remainder}}. \quad (6)$$

The hedge demand can be decomposed into three different sources (disregarding the residual term), as seen by the first three terms of Equation (5) and (6). First, in order to have a position with a maturity of 30 days, the issuer holds a portfolio of the first- and second-months futures in proportions yielding an average maturity of 30 days. As each

of these contracts gets closer to expiry, the position in the first-month contract must be decreased, and the position in the second-month contract must be increased (assuming the ETP has a long exposure). This is denoted as calendar rebalance. Second, leveraged and inverse products must rebalance as the underlying changes in order to keep their leverage at the target. This mechanism induces both leveraged and inverse ($L<0$) ETPs to be selling (buying) as the benchmark index decreases (increases), equivalent of having a short gamma exposure in options. Appendix B provides an illustrative example of this mechanism. The final part of the hedging demand is due to capital inflow or outflow of the ETP. Demand in both VX1 and VX2 is increasing with this flow component. Thus, all else equal, inflows (outflows) generate a buying (selling) pressure from VIX ETPs. An important remark is that most of the VIX ETPs are exchange traded notes (ETNs), which, unlike exchange traded funds (ETFs), are not required to hold the underlying assets. Hence the issuer of an ETN can choose to hedge in VIX futures further out on the term structure (due to cost considerations), other types of derivatives, or not to hedge at all.[10]

The total dollar demand of all N ETPs in the market is given by: $D^{\$,all}_{t,VX1} = \sum_{j=1}^{N} D^{\$,j}_{t,VX1}$, $D^{\$,all}_{t,VX2} = \sum_{j=1}^{N} D^{\$,j}_{t,VX2}$.

The growth of the VIX ETP market has been a main driver of the increased liquidity in the VIX Futures. However, concerns have been raised that the products are susceptible to causing feedback dynamics in the entire VIX complex and have become the "tail wagging the dog." This is due to the large size of the ETPs relative to the market for VIX futures, which underlies the products. Illustrating this concern, Figure VII, Panel (a) shows the hedging demand for the two front-month VIX futures, VX1 and VX2, measured in number of futures contracts relative to the OI. Assuming that all VIX ETPs are 100% hedged via VIX futures, their demand occasionally absorbs substantial shares of the entire futures market. This is particularly pronounced at the Volmagedon event, February 5, 2018, where the combined demand of all VIX ETPs made up 79% and 80% of the OI in VX1 and VX2, respectively.

[10] As anecdotal evidence, this was the case for the inverse product SVXY during the volmagedon event, see e.g., Bloomberg (2018).

Inevitably, demand of this magnitude will have a pricing impact on the VIX futures. Panel (b) shows the decomposition of the hedging demand throughout my sample period, combined for VX1 and VX2. Demand is in absolute values. Calendar rebalance makes up a large fraction, with 40% of the total demand on average. Leverage rebalance is, on average, much lower (24%) but tends to spike in certain periods. For instance, on February 5, 2018, leverage rebalance makes up 90% of the demand, and 99% at the end of August 2015. In general, we see that the contribution from this source tends to cluster around periods of increased volatility (August 2015, February 2018, March 2020), where the returns on the underlying benchmark index of VIX ETPs are large in magnitude. The contribution from flow rebalancing is quite consistent through the sample and makes up 30% on average. Finally, we can note that the remainder term of Equations (5) and (6) is very small (on average 2.6%).

The leverage targeting of inverse and leveraged ETPs is of particular concern as this may cause feedback loops that destabilize not only the VIX futures market but also the market for SPX options that underlie the VIX. Figure VIII illustrates the potential feedback mechanism in the VIX complex. A negative shock to the stock market is the catalyst. In reach for protection, market participants will buy up the price of SPX put options whereby the VIX will increase by construction. As the VIX is the underlying of VIX futures, the VIX futures prices will naturally rise as well, yielding a positive return in the underlying benchmark index of VIX futures that the ETPs track. From Equations (5) and (6), the leverage rebalance is increasing in the returns of the benchmark, hence leveraged and inverse products will need to buy more VIX futures in order to maintain their leverage target. Furthermore, this demand is also increasing in the AUM of the ETP. Hence, large products will likely have a pricing impact, driving the VIX futures prices further up. Then again, due to the leverage target, they need to buy even more, etc. So there is clearly a potential feedback mechanism between VIX ETPs and VIX futures. However, we may also have spillover effects on the SPX options market. The market maker on the other side of the ETP demand will have a short vega position (i.e., lose money of volatility increases) from selling VIX futures. If the capacity in

Figure VII: VIX ETP hedge demand

Figure VII shows the theoretical hedge demand for VIX futures from VIX ETPs throughout my sample. Panel (a) shows the number of contracts relative to the total open interest in VIX futures for the first and second-month contracts (VX1 and VX2). Panel (b) shows decomposition of the total demand in absolute values.

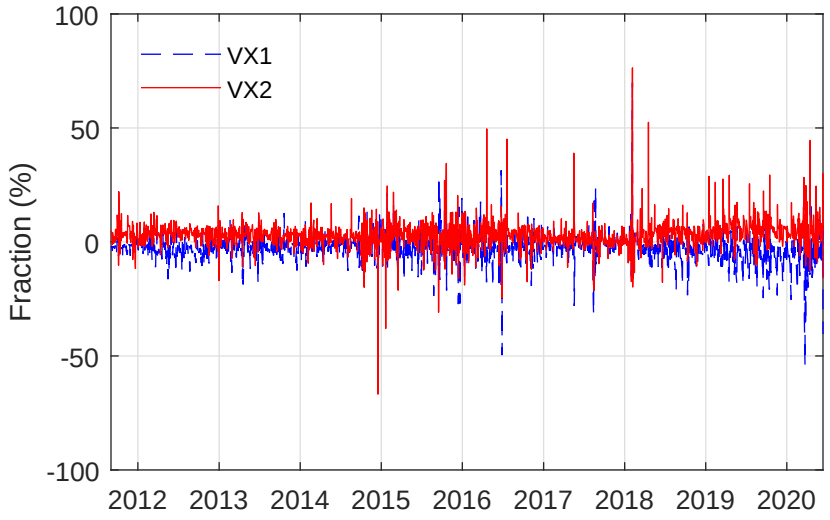

(a) Hedge demand relative to OI

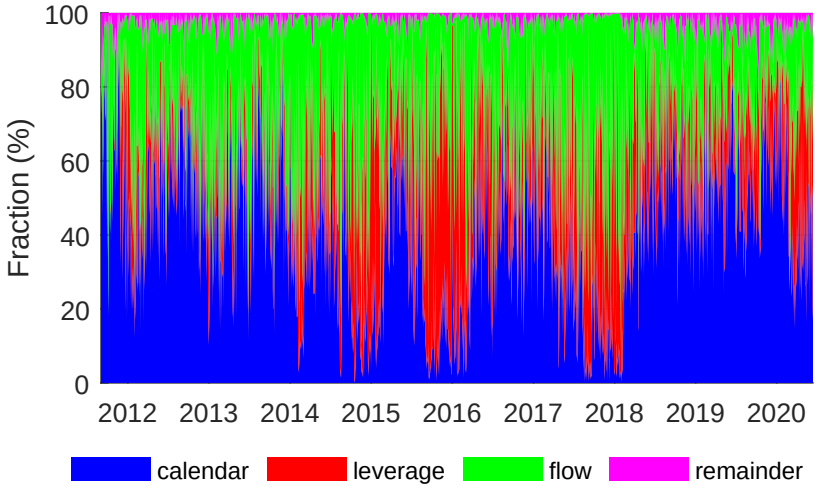

(b) Decomposition of ETP hedge demand

Figure VIII: Potential feedback dynamics in the VIX-complex.

Figure VIII illustrates the potential feedback mechanism of the VIX complex.

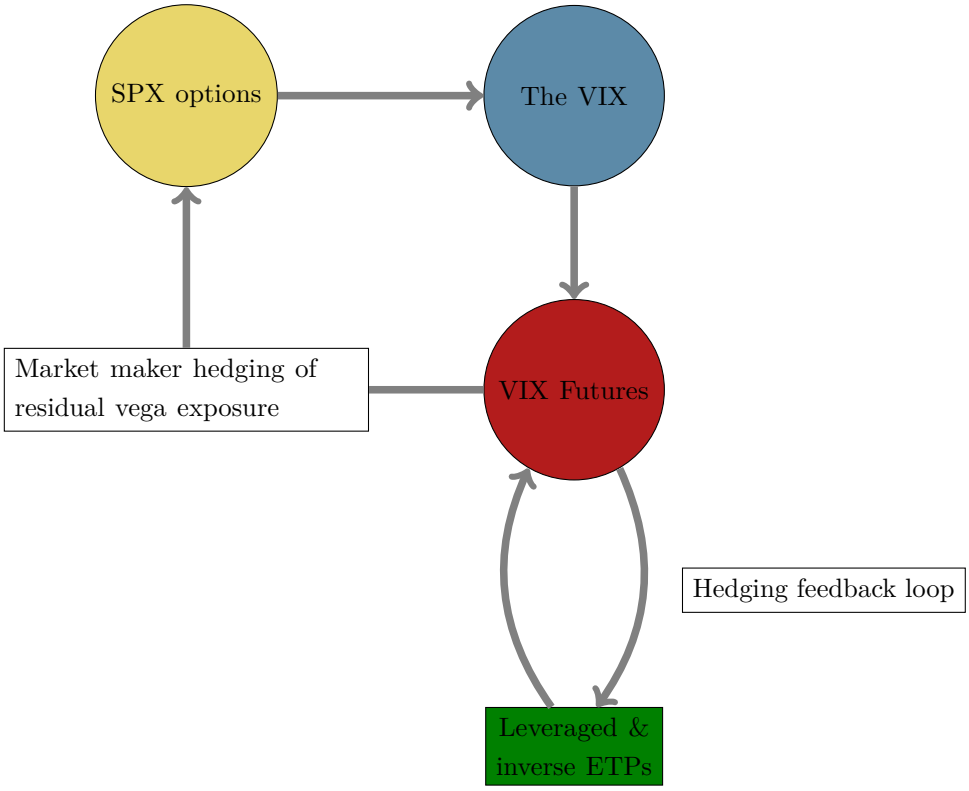

the market for VIX futures is exhausted, she may choose to hedge this via the SPX options that enter the VIX calculation instead. In a stressed market, this may drive up the price of SPX options and thereby cause a further increase in the VIX, which will feed over into the VIX futures, which then again induce further buying on the leveraged and inverse ETPs. So what initially may seem like a small spike in the volatility or the VIX can potentially be severely amplified by these rebalancing mechanisms of leveraged and inverse ETPs. It seems to be the widespread belief that these dynamics are what caused the Volmagedon event on February 5, 2018, where the entire VIX complex blew, up and XIV generated a 90% loss of value.

III.B. The VIX complex model: Specification and estimation

I investigate the dynamics of the VIX complex by expanding the state space model in Section II.C with two additional variables. Specifically, I include the VIX and a demand variable (standardized to mean zero and unit variance). I define the demand variable as:

$$Demand_t = \frac{D^{\$,all}_{t,VX1}/(m \times \text{VX1}_t)}{\text{OI}^{VX1}_t} + \frac{D^{\$,all}_{t,VX2}/(m \times \text{VX2}_t)}{\text{OI}^{VX2}_t}, \tag{7}$$

with m being the contract multiplier and OI^{VX1}_t (OI^{VX2}_t) is the OI of VX1 (VX2), at time t. The numerator of each term is the dollar demand converted into number of contracts. Thus each term is the demand relative to the total size of the market for the specific futures contract. Thereby I isolate the effect of a larger share of ETP demand from a pure increase in the size of the overall market as in Todorov (2020).

The state vector now becomes $\boldsymbol{\beta}_t = (\text{VIX}_t, \text{Level}_t, \text{Slope}_t, \text{Curvature}_t, \text{Demand}_t)'$, in that order. The dimensions of $\boldsymbol{\Phi}$, $\boldsymbol{\mu}$, $\mathbf{R}$, and $\mathbf{Q}$ are increased as appropriate.[11] By this particular recursive causal ordering of the state vector, I am assuming that a shock first occurs in the VIX, in line with the dynamics of the VIX complex described above.

As I only consider demand in VX1 and VX2, I am disregarding the potential pricing impacts stemming from the mid-term ETPs. But given the small size of this product segment, it seems fair to assume that short-term ETPs are the main source of price distortions.

I collect the daily VIX close from CBOE. Daily AUM and prices of the VIX ETPs alive during my sample are collected from Bloomberg. From these two series, I calculate daily capital flows, following the procedure in Barber et al. (2016).

Panel A of Table IV displays the parameter estimates of $\boldsymbol{\Phi}$ and $\boldsymbol{\mu}$.[12] First of all, we note that the VIX is very persistent with an own-lag coefficient of 0.99. The cross-factor dynamics for the VIX and the other variables are all insignificant. Hence there appear to be no spill-over effects from the other variables to the VIX. The mean level of the VIX is

[11] Appendix III.A provides details on how the state space system is specified for the VIX complex model.
[12] Stationarity is assured since all eigenvalues of $\boldsymbol{\Phi}$ are below 1.

16.63, reflecting the run-up in stock prices over the sample period. Panel B contains the upper diagonal coefficients of the matrix $\mathbf{Q}$. Not surprisingly, all the off-diagonal elements are significant, implying correlated shocks. Finally, the estimate of the loading parameter, λ, is 0.0149.

Table IV: Parameter estimates of the VIX complex model

Table IV reports the estimates of the parameter coefficients of the expanded state space model. Panel A reports the VAR coefficient matrix $\boldsymbol{\Phi}$ and the mean vector $\boldsymbol{\mu}$. Panel B reports the coefficients of the variance matrix $\boldsymbol{Q}$. The recursive causal ordering of the state variables is VIX, Level, Slope, Curvature, and Demand. Standard errors are given in parenthesis. ** and * represents significance at 1% and 5%, respectively.

Panel A: Estimates of Φ matrix and μ vector

	VIX_{t-1}	Level_{t-1}	Slope_{t-1}	Curvature_{t-1}	Demand_{t-1}	μ
VIX_t	0.99**	0.00	-0.02	-0.01	-0.05	16.63**
	(0.03)	(0.03)	(0.03)	(0.01)	(0.04)	(1.20)
Level_t	0.01	0.98**	-0.02	0.02**	-0.06	22.12**
	(0.02)	(0.02)	(0.02)	(0.00)	(0.04)	(1.46)
Slope_t	0.17**	-0.19**	0.80**	-0.03**	-0.04	-5.26**
	(0.03)	(0.03)	(0.03)	(0.00)	(0.03)	(0.77)
Curvature_t	-0.06*	0.06	0.11**	0.96**	0.28**	-1.43
	(0.03)	(0.04)	(0.04)	(0.01)	(0.08)	(1.47)
Demand_t	-0.08**	0.08**	0.07**	0.00	-0.00	0.00
	(0.02)	(0.02)	(0.02)	(0.00)	(0.01)	(0.00)

Panel B: Estimate of Q matrix

	VIX_t	Level_t	Slope_t	Curvature_t	Demand_t
VIX_t	6.54**	1.35**	3.72**	-4.93**	1.80**
	(0.11)	(0.06)	(0.10)	(0.14)	(0.06)
Level_t		0.78**	0.08**	-2.21**	0.24**
		(0.03)	(0.04)	(0.08)	(0.04)
Slope_t			3.54**	-1.06**	1.60**
			(0.09)	(0.09)	(0.05)
Curvature_t				7.33**	-1.11**
				(0.24)	(0.09)
Demand_t					1.96**
					(0.03)

The time-series estimates of the level, slope, and curvature factors are very similar to those obtained in the futures-only model, see Appendix III.B. Thus, as shown in the second and third columns of Table V, the means and standard deviations of the measurement errors are almost identical to those of the VIX futures-only model and are small in magnitude.

Table V: Summary statistics of measurement errors - VIX complex model

Futures contract	Mean	Standard deviation
VX1	-0.03	0.19
VX2	0.04	0.25
VX3	0.02	0.19
VX4	-0.04	0.17
VX5	-0.03	0.24
VX6	-0.01	0.25
VX7	0.02	0.19
VX8	0.02	0.21

III.C. VIX complex impulse response functions

I examine the dynamics of the VIX complex via impulse response functions, which are depicted in Figure IX, along with 95 percent confidence bands. The shocks are orthogonalized using a Cholesky decomposition of the variance matrix $\mathbf{Q}$. Time is measured in days after the shock. First, consider the responses to a shock in the VIX. The level factor increases sharply and shows a significant level of persistence. This implies that VIX spikes increase the entire term structure, which remains elevated for the period following, in line with the typical clustering of market volatility. A VIX shock also increases the slope factor. As a negative slope factor equals an upward-sloping term structure, the slope thus decreases with the VIX shock, implying an inverted term structure for high VIX values. This effect is also very persistent, implying that the term structure tends to stay in backwardation for several days following a VIX spike. The curvature factor decreases and is also rather persistent, but the effect seems to die out slightly faster than for the level and slope factors. After ten days, zero is included within the confidence band. Finally, a shock to the VIX increases the demand variable. The benchmark index of the ETPs will have large positive returns when the VIX increases, and, consequently, leveraged and inverse products must buy VIX futures to maintain the leverage target. However, there is a quick reversal. This is in line with the empirical fact that spikes in the VIX are typically followed by large capital outflows, as documented in Nielsen and Posselt (2020). These outflows will induce the issuers to reduce their hedge positions in VIX futures, whereby demand decreases. Next, we look at

the responses to a shock in demand. First, we see that demand quickly reverses following the shock. Second, the VIX is clearly unaffected at all horizons. Thus my results provide no evidence of VIX futures demand from ETPs impacting the VIX. We detect a small decrease in the level factor, but it is not statistically significant. There is no response in the slope factor. The curvature factor, on the other hand, increases at time t+1, with zero not included in the confidence band. Two likely explanations could be the following; Consider the empirical proxy of the curvature factor $2 \times$ VX3-(VX1+VX8). An increased curvature could be due to an increase in the price of VX3, which would indicate that the issuers of VIX ETPs are also hedging their exposure via VIX futures further out on the term structure. These typically have a lower decay in value than the front-month contracts and are thereby "cheaper" to hold. A second explanation could be that demand quickly reverses following a shock for instance due to capital outflows. Consequently, the issuers will reduce their position in VX1, resulting in downward price pressure, whereby the curvature increases. This explanation would support the hypothesis in Nielsen and Posselt (2020), which suggests that the VIX premium puzzle of Cheng (2019) is caused by VIX ETP investors betting on mean reversion of the VIX. In either case, rise in curvature following the demand shocks indicates that the hedging activity of ETPs impacts the VIX futures term structure.

Next, we focus on shocks to the different term structure factors. The VIX has no response to either of the factors. The level factor is quite persistent as it reverts very slowly following the shock. The response to the slope factor is negative, implying an increased slope of the term structure. Recalling the empirical proxy for the slope, VX8 - VX1, the increase in the slope likely follows from the increase in VX8, which proxies for the level factor. The curvature factor also has a negative response. Again this follows intuitively from the empirical proxy, which is decreasing in the long term level, VX8. The demand variable also decreases in response to the level shock. This could suggest that the front month futures, VX1 and VX2, tend to decrease when the long term level increases, as the issuer demand is increasing in the returns of these contracts. A shock to the slope factor increases the demand variable. An

increased slope factor implies an inverted term structure, with large increases in VX1 and VX2, which then, in turn, increases the hedging demand. Finally, a shock to the curvature factor leads slowly to an increase in the level factor and a time t=0 decrease in demand, which reverts very quickly.

Figure IX: Impulse responses of the VIX complex model

Figure IX shows the responses down the rows to the shocks of each variable along the columns. The shocks have been orthogonalized by means of a Cholesky decomposition of the variance matrix **Q**. The recursive causal ordering of the state variables is VIX, Level, Slope, Curvature, and Demand.

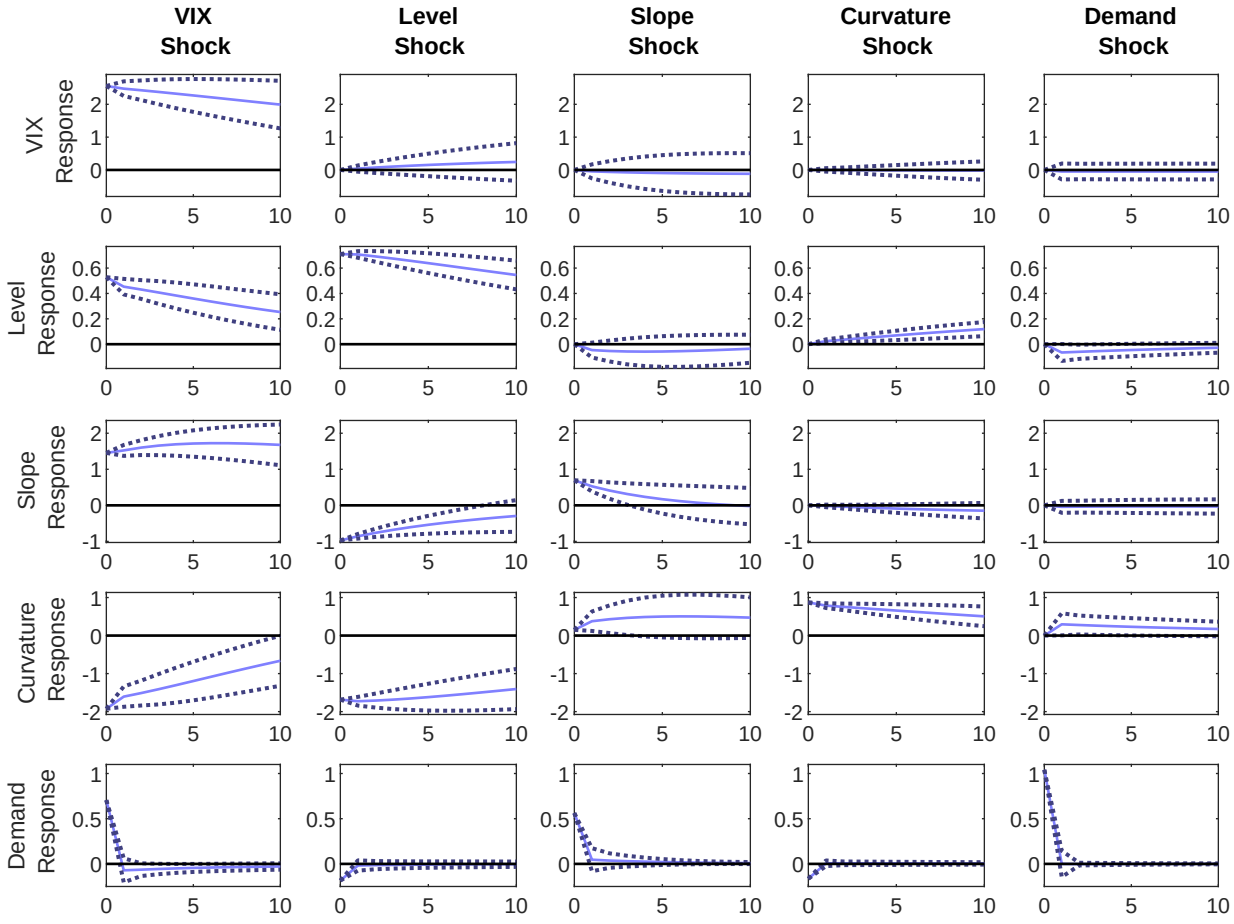

III.D. Variance decomposition of VIX futures, the VIX and demand

As a final analysis, I make variance decompositions for analyzing the interactions of the VIX complex. These are calculated following the appendix of Diebold et al. (2006), assuming a non-diagonal variance matrix, **Q**. Panel A of Table VI provides a variance decomposition of the VIX futures contracts, VX1, VX4, and VX8 (representing the front, middle and long end of the VIX futures term structure) at forecast horizons of 1, 5 and 10 days based on the VIX futures-only model. Across all the contracts, the main contribution to variation is either from the level or slope factor. Curvature seems to be of minor importance. But if we then consider the variance decomposition based on the VIX complex model, provided in Panel B, much of the variation in the futures prices attributed to the level or slope factor is now traced to the VIX. For example, in the VIX futures-only model for VX1 at a one-day horizon, 18% and 81% of the price variation is accounted for by the level and slope factor, respectively. In the VIX complex model, these are 3% and 10%, whereas the VIX accounts for 87%. However, for VX8, the effect is the opposite of the curvature factor. The contribution has increased slightly in the VIX complex model compared to the VIX futures-only model (from 14% to 15%).

In the VIX complex model, we see that across all contracts, the majority of the variance contribution is from the VIX. However, a non-negligible part can still be traced to the slope factor. This matches very well with Johnson (2017), who finds that the second principal component of the VIX term structure (not to be confused with the term structure of VIX futures) explains much of the variation in returns of different volatility assets. VIX futures tend to roll down the term structure as they get closer to expiry, and the slope can be regarded as an estimate of how large the price decay will be. The steeper the slope, the larger is the expected decay. In light of this, the slope can be regarded as variance risk premium paid by the buyer of a VIX futures contract.

Panel B also contains the variance decomposition of the VIX and the demand variable. For the VIX at horizon 1 and 5 days, all the variation is entirely driven by itself. However, at

the 10-day horizon, the level factor accounts for 1% of the variance. This indicates that for very low (high) levels, the VIX tends to revert upwards (downwards) to the long-term level, thus reflecting the typical mean-reverting nature of the VIX. Also, for the demand variable, the VIX is a large contributor (26% at all horizons), but the slope factor also drives much of the variation with 16% at all horizons. A steep positive slope (high contango) would mean a large variance risk premium, and thereby a large roll-down of the VIX futures, decreasing the return of the benchmark index. This will, in turn, decrease the demand from ETPs. In the case of a steep negative slope (high backwardation), the process is reversed. The benchmark index will have high positive returns inducing an increased demand from ETPs.

Table VI: Variance decomposition

Table VI shows the variance decomposition of the VIX futures contracts VX1, VX4, and VX8 from the VIX futures-only model in Panel A and the VIX complex model in Panel B. Furthermore, Panel B also contains the variance decomposition of the VIX and demand.

	Horizon	VIX	Level	Slope	Curvature	Demand
Panel A: Futures-only model						
VX1	1	–	0.18	0.81	0.01	–
	5	–	0.21	0.78	0.00	–
	10	–	0.25	0.75	0.00	–
VX4	1	–	0.31	0.54	0.16	–
	5	–	0.34	0.54	0.12	–
	10	–	0.38	0.53	0.09	–
VX8	1	–	0.64	0.22	0.14	–
	5	–	0.66	0.22	0.12	–
	10	–	0.67	0.22	0.11	–
Panel B: VIX complex model						
VX1	1	0.87	0.03	0.10	0.00	0.00
	5	0.94	0.01	0.05	0.00	0.00
	10	0.96	0.01	0.03	0.00	0.00
VX4	1	0.66	0.09	0.17	0.08	0.00
	5	0.78	0.05	0.10	0.07	0.00
	10	0.85	0.03	0.06	0.06	0.00
VX8	1	0.70	0.00	0.15	0.15	0.00
	5	0.77	0.01	0.09	0.13	0.00
	10	0.80	0.02	0.06	0.12	0.00
VIX	1	1.00	0.00	0.00	0.00	0.00
	5	1.00	0.00	0.00	0.00	0.00
	10	0.99	0.01	0.00	0.00	0.00
Demand	1	0.26	0.02	0.16	0.01	0.55
	5	0.26	0.02	0.16	0.01	0.55
	10	0.26	0.02	0.16	0.01	0.55

IV. Conclusion

The interactions between the VIX, VIX futures and VIX ETPs have received much attention. Concerns have been raised that the hedging activities of the issuers of VIX ETPs impacts the pricing of VIX futures and potentially also the VIX, leading to a "tail wagging the dog" effect. By means of the Dynamic Nelson-Siegel (DNS) model estimated in a state space framework, I first show that the VIX futures term structure is well described by the three latent factors, Level, Slope, and Curvature. The estimated model produces very low pricing errors.

The state space model is expanded with two additional variables; The VIX and a proxy for the VIX futures demand from issuers of VIX ETPs. Thereby I model the VIX complex as a nonstructural VAR(1) system. Similar to the VIX futures-only model, the expanded model fits the VIX futures term structure quite well, with low pricing errors. The dynamics of the VIX complex are examined via impulse response functions. Not surprisingly, a shock to the VIX raises the level of the VIX futures term structure and decreases the slope (inverting the term structure). Furthermore, hedge demand for ETP issuers also increases, as they must buy (sell) when the VIX futures prices increases (decreases). I find no evidence of effects from VIX futures or demand to the VIX. However, a shock to demand increases the curvature of the VIX futures term structure, suggesting that the hedging of VIX ETPs do have pricing impacts that distort the VIX futures market. Finally, a variance decomposition shows that the VIX and the slope factor are the main drivers of the variation in the prices of VIX futures.

References

Barber, B. M., X. Huang, and T. Odean (2016). Which Factors Matter to Investors? Evidence from Mutual Fund Flows. *Review of Financial Studies 29*(10), 2600–2642.

Ben-David, I., F. Franzoni, and R. Moussawi (2018). Do etfs increase volatility? *Journal of Finance 73*(6), 2471–2535.

BIS (2018). Bank for international settlements quarterly review - march 2018.

Bloomberg (2018). https://www.bloomberg.com/opinion/articles/2018-02-09/inverse-volatility-products-almost-worked. Last accessed: December, 2020.

Bloomberg (2019). https://www.bloomberg.com/news/articles/2019-02-06/the-day-the-vix-doubled-tales-of-volmageddon. Last accessed: December, 2020.

Bollen, N. P. B., M. J. O'Neil, and R. E. Whaley (2017). Tail Wags Dog: Intraday Price Discovery in VIX Markets. *Journal of Futures Markets 37*(5), 431–451.

Brenner, M. and D. Galai (1989). New Financial Instruments for Hedge Changes in Volatility. *Financial Analysts Journal 45*(4), 61–65.

Brøgger, S. B. (2020). The market impact of predictable flows: Evidence from leveraged vix products. *Working paper*.

Chen, Y., Q. Han, and L. Niu (2018). Forecasting the term structure of option implied volatility: The power of an adaptive method. *Journal of Empirical Finance 49*(1), 157–177.

Chen, Y.-L. and W.-C. Tsai (2017). Determinants of price discovery in the vix futures market. *Journal of Empirical Finance 43*, 59–73.

Cheng, I.-H. (2019). The VIX Premium. *Review of Financial Studies 32*(1), 180–227.

Cheng, M. and A. Madhavan (2009). The dynamics of leveraged and inverse exchange-traded funds. *Working paper*.

Diebold, F. X. and C. Li (2006). Forecasting the term structure of government bond yields. *Journal of Econometrics 130*(2), 337–364.

Diebold, F. X., G. D. Rudebusch, and S. Aruoba (2006). The macroeconomy and the yield curve: a dynamic latent factor approach. *Journal of Econometrics 131*(1), 309 – 338.

Fernandez-Perez, A., B. Frijns, A. Tourani-Rad, and R. I. Webb (2019). Does increased hedging lead to decreased price efficiency? The case of VIX ETPs and VIX futures. *Financial Review 54*, 477–500.

Frijns, B., A. Tourani-Rad, and R. I. Webb (2016). On the Intraday Relation Between the VIX and its Futures. *Journal of Futures Markets 36*(9), 870–886.

Golez, B. and J. C. Jackwerth (2012). Pinning in the s&p 500 futures. *Journal of Financial Economics 106*, 566–585.

Granger, C. W. J. (1969). Investigating Causal Relations by Econometric Models and Cross-spectral Methods. *Econometrica 37*(3), 424–438.

Griffin, J. M. and A. Shams (2018). Manipulation in the VIX? *Review of Financial Studies 31*(4), 1377–1417.

Grønborg, N. S. and A. Lunde (2016). Analyzing Oil Futures with a Dynamic Nelson-Sigel Model. *Journal of Futures Markets 36*(2), 153–173.

Guo, B., Q. Han, and H. Lin (2017). Are there gains from using information over the surface of implied volatilities. *Journal of Futures Markets 38*(6), 645–672.

Guo, B., Q. Han, and B. Zhao (2014). The nelson-siegel model of the term structure of option implied volatility and volatility components. *Journal of Futures Markets 34*(8), 788–806.

Hamilton, J. D. (1994). *Time Series Analysis* (2 ed.). Princeton University Press.

Hansen, N. and A. Ostermeier (1996). Adapting arbitrary normal mutation distributions in evolution strategies: The covariance matrix adaption. *Proceedings of IEEE International Conference on Evolutionary Computation*, 312–317.

Ivanov, I. T. and S. L. Lenkey (2018). Do leveraged etfs really amplify late-day returns and volatility? *Journal of Financial Markets 41*, 36–56.

Johnson, T. L. (2017). Risk premia and the vix term structure. *Journal of Financial and Quantitative Analysis 52*(6), 2461–2490.

Koopman, S. J., M. I. P. Malle, and M. van der Wel (2010). Analyzing the term structure of interest rates using the dynamic nelson-siegel with time-varying parameters. *Journal of Business & Economic Statistics 28*(3), 329–343.

Menacía, J. and E. Sentana (2013). Valuation of vix derivatives. *Journal of Financial Economics 108*(2), 367–391.

Mixon, S. and E. Onur (2015). Volatility derivatives in practice: Activity and impact. *Working paper*.

Nelson, C. R. and A. F. Siegel (1987). Parsimonious modeling of yield curves. *Journal of Business 60*(4), 473–489.

Ni, S. X., N. D. Pearson, and A. M. Poteshman (2005). Stock price clustering on option expiration dates. *Journal of Financial Economics 78*, 49–87.

Ni, S. X., N. D. Pearson, A. M. Poteshman, and J. White (2021). Does option trading have a pervasive impact on underlying stock prices? *Review of Financial Studies 34*(6), 1952–1986.

Nielsen, O. L. and A. M. Posselt (2020). Betting on mean reversion in the vix? evidence from the revealed preferences of investors. *Working paper*.

Schum, P., W. Hejazi, E. Haryanto, and A. Rodier (2016). Intraday share price volatility and leveraged rebalancing. *Review of Finance 20*(6), 2379–2409.

Shu, J. and J. E. Zhang (2012). Causality in the vix futures market. *Journal of Futures Markets 32*(1), 24–46.

Todorov, K. (2020). Passive funds actively affect prices: Evidence from the largest etf markets. *Working Paper*.

West, J. (2012). Long-dated agricultural futures price estimates using the seasonal nelson-siegel model. *International Journal of Business and Management 7*(3), 78–93.

Whaley, R. E. (1993). Derivatives on market volatility: Hedging tools long overdue. *Journal of Derivatives 1*(1), 71–84.

Whaley, R. E. (2009). Understanding the vix. *Journal of Portfolio Managment 35*(3), 98–105.

A. Estimation based on the Kalman filter

Denote $\hat{\boldsymbol{\beta}}_{t|s}$ as the linear least square forecast of the state vector, $\boldsymbol{\beta}_t$, given observations $\mathbf{y_1}, ..., \mathbf{y_s}$ with mean square error (MSE) matrix, $\mathbf{P}_{t|s}$, for $s{=}t-1$, t. Then, when observation $\mathbf{y_t}$ becomes available, the Kalman filter computes $\hat{\boldsymbol{\beta}}_{t|t}$ and $\mathbf{P}_{t|s}$ as (the filtering step):

$$\begin{aligned} \hat{\boldsymbol{\beta}}_{t|t} &= \hat{\boldsymbol{\beta}}_{t|t-1} + \mathbf{P}_{t|t-1}\boldsymbol{\Lambda}(\lambda)'\mathbf{F}_t^{-1}\mathbf{v}_t, \\ \mathbf{P_{t|t}} &= \mathbf{P_{t|t-1}} - \mathbf{P_{t|t-1}}\boldsymbol{\Lambda}(\lambda)'\mathbf{F}_t^{-1}\mathbf{P_{t|t-1}}, \end{aligned} \tag{8}$$

where $\mathbf{v}_t = \mathbf{y}_t - \hat{\mathbf{y}}_{t|t-1} = \mathbf{y}_t - \boldsymbol{\Lambda}(\lambda)\hat{\boldsymbol{\beta}}_{t|t-1}$ is the forecast error vector and $\mathbf{F}_t = \boldsymbol{\Lambda}(\lambda)\mathbf{P_{t|t-1}}\boldsymbol{\Lambda}(\lambda)' + \mathbf{R}$ is he forecast error variance matrix. The $t+1$ forecast of the state vector conditional on $\mathbf{y_1}, ..., \mathbf{y_t}$, is provided by the prediction step:

$$\begin{aligned} \hat{\boldsymbol{\beta}}_{t+1|t} &= (\mathbf{I} - \boldsymbol{\Phi})\boldsymbol{\mu} + \hat{\boldsymbol{\beta}}_{t|t}, \\ \mathbf{P_{t+1|t}} &= \boldsymbol{\Phi}\mathbf{P_{t|t}}\boldsymbol{\Phi}' + \mathbf{Q}. \end{aligned} \tag{9}$$

Then, by updating the system of Equation (8) and Equation (9) recursively for $t = 1, ..., T$ I obtain a time series of the latent factors (Level, Slope, and Curvature) of the VIX futures term structure.

I initialize the Kalman filter using the unconditional mean of the state vector (0) and the unconditional covariance matrix of the state vector, $\boldsymbol{\Sigma}_\beta$ which is chosen such that $\boldsymbol{\Sigma}_\beta - \boldsymbol{\Phi}\boldsymbol{\Sigma}_\beta\boldsymbol{\Phi}' = \mathbf{Q}$.[13] To solve for $\boldsymbol{\Sigma}_\beta$, apply the vectorization operator to both sides and obtain:

$$vec(\boldsymbol{\Sigma}_\beta) - vec(\boldsymbol{\Phi}\boldsymbol{\Sigma}_\beta\boldsymbol{\Phi}') = vec(\mathbf{Q}). \tag{10}$$

[13]This enables the Kalman filter to provide a minimum mean squared error estimate of $\boldsymbol{\beta}_t$ at every time $t = 1, ... , T$ given information up to time $t-1$. See Hamilton (1994) or Koopman et al. (2010)

Rewrite this as:

$$\mathbf{I}vec(\mathbf{\Sigma_\beta}) - (\mathbf{\Phi} \otimes \mathbf{\Phi}vec(\mathbf{\Sigma_\beta}) = (\mathbf{I} - (\mathbf{\Phi} \otimes \mathbf{\Phi}))vec(\mathbf{\Sigma_\beta}) = vec(\mathbf{Q}), \tag{11}$$

where $\mathbf{I}$ is the identity matrix with dimension $n \times n$, with n being the number of state variables. The final solution for $vec(\mathbf{\Sigma_\beta})$ is then given by:

$$vec(\mathbf{\Sigma_\beta}) = (\mathbf{I} - (\mathbf{\Phi} \otimes \mathbf{\Phi}))^{-1}vec(\mathbf{Q}). \tag{12}$$

B. Rebalance dynamics of inverse and leveraged ETPs

Consider the example of a leveraged ETP that promises 2x the returns of the underlying, X. The ETP initially issues 100,000 shares at a price of \$100 (initial AUM of \$10 mm.), borrows an additional \$10 mm. and invest all the proceeds in the underlying, X, at a price of 400 whereby the ETP holds 50,000 shares. Table VII illustrates the effective leverage of the ETP through time as X varies. At time 1, X, yields a return of 5%, and the return of the ETP is 10%. Thus a return of the desired leverage is obtained. But for the subsequent periods, the ETP fails to achieve its target of 2. The problem is that the AUM of the ETP changes. In this case, it went up while the amount of debt is constant. So following an increase in the underlying, the 2x leveraged ETP must buy additional shares in X, worth of the percentage change in the ETP times the AUM at time $t-1$, using additional leverage.

Table VIII illustrates how the leveraged ETP must rebalance the amount of debt and the position in X through time in order to keep the leverage constant at 2. At time 1, following the increase in the underlying, the ETP must buy an additional 2,381 shares in X by raising \$1,000,020 of extra debt. To minimize the tracking error, the purchase of these shares will be done near the market close or in the after-market.

Consider next the example of an ETP that promises the inverse of the return of X. Thus, the desired leverage of the ETP is now -1. Again the ETP initially issues 100,000 shares at a

Table VII: Performance of leveraged ETP that does not rebalance

Table VII shows the development of the leverage ratio through time for a leveraged ETP that does not rebalance the number of shares it holds in the underlying. The second column shows the value development of the underlying that the ETP tracks. The third column shows the return of the underlying, and the fourth column is the NAV of the ETP calculated as # of shares multiplied by X_t + Cash (last column), all divided by the number of outstanding shares in the ETP (seventh column). The fifth column shows the return of the ETP, and the sixth contains the leverage through time, calculated as return of the ETP divided by the return of the underlying. Column six is the asset under management (AUM) of the ETP, calculated as outstanding shares in the ETP multiplied by the NAV. Column seven is the number of shares that the ETP holds in the underlying at the start of the day. Column eight is the number of shares that the ETP buys or sells at the end of the trading day.

Time	X_t	r_t^X	NAV_t	r_t^{ETP}	Leverage_t	ETP shares	AUM	# shares	Δ shares	Cash
0	400	-	100	-	-	100,000	$ 10,000,000	50,000	-	$ -10,000,000
1	420	5%	110	10%	2.0	100,000	$ 11,000,000	50,000	-	$ -10,000,000
2	428	2%	114	3.8%	1.9	100,000	$ 11,420,000	50,000	-	$ -10,000,000
3	386	-10%	93	-19%	1.9	100,000	$ 9,278,000	50,000	-	$ -10,000,000
4	424	10%	112	21%	2.1	100,000	$ 11,205,800	50,000	-	$ -10,000,000
5	450	6%	125	11%	1.9	100,000	$ 12,478,148	50,000	-	$ -10,000,000

price of $100. Then it sells short 25,000 shares in X and deposits all the proceeds (investor capital + proceeds from short sale) in a bank account. Table IX shows effective leverage through time if the ETP does not rebalance.

At time 1, the return of X is 5%, and for the ETP, it is -5%, so the desired leverage is initially obtained. But then, as X increases further in value, the short exposure also increases. This is because the AUM of the ETP has decreased, but the value of the shorted shares has increased. Thus, the ETP now has too many short shares outstanding relative to the AUM. Thus following an increase in the underlying and inverse ETP must cover a part of the short position by buying back shares, using some of the cash that initially was deposited in the bank account. Likewise, in case of a decrease in the underlying, the inverse ETP must short an additional amount of shares, or the short exposure will be lower than the target.

For both leveraged and inverse ETPs the number of shares to either sell or buy in order to maintain the leverage is given by:

$$\Delta \text{ shares} = \frac{L \times (L-1) \times r_t^X \times \text{AUM}_{t-1}}{X_t}. \tag{13}$$

Table VIII: Performance of leveraged ETP that rebalances

Table VIII shows the development of the leverage ratio through time for a leveraged ETP that rebalances the number of shares it holds in the underlying. The second column shows the value development of the underlying that the ETP tracks. The third column shows the return of the underlying, and the fourth column is the NAV of the ETP calculated as # of shares multiplied by X_t + Cash (last column), all divided by the number of outstanding shares in the ETP (seventh column). The fifth column shows the return of the ETP, and the sixth contains the leverage through time, calculated as return of the ETP divided by the return of the underlying. Column six is the asset under management (AUM) of the ETP, calculated as outstanding shares in the ETP multiplied by the NAV. Column seven is the number of shares that the ETP holds in the underlying at the start of the day. Column eight is the number of shares that the ETP buys or sells at the end of the trading day.

Time	X_t	r_t^X	NAV$_t$	r_t^{ETP}	Leverage$_t$	ETP shares	AUM	# shares	Δ shares	Cash
0	400	-	100	-	-	100,000	$ 10,000,000	50,000	-	$ -10,000,000
1	420	5%	110	10%	2.0	100,000	$ 11,000,000	50,000	2,381	$ -11,000,020
2	428	2%	114	4%	2.0	100,000	$ 11,440,000	52,381	1,028	$ -11,440,415
3	386	-10%	93	-20%	2.0	100,000	$ 9,151,959	53,409	-5,934	$ -9,152,502
4	424	10%	110	20%	2.0	100,000	$ 10,982,405	47,475	4,316	$ -10,982,987
5	450	6%	123	12%	2.0	100,000	$ 12,300,328	51,791	2,932	$ -10,000,000

Table X shows how many shares that the inverse ETP must buy and sell through time to maintain leverage of -1. Note that the ETP always buys and sells in the direction of X. This is also the case for the leveraged ETP. Thus both leveraged and inverse ETPs must buy (sell) whenever the underlying increases (falls) in value.

Table IX: Performance of inverse ETP that does not rebalance

Table IX shows the development of the leverage ratio through time for an inverse ETP that does not rebalance the number of shares it holds in the underlying. The second column shows the value development of the underlying that the ETP tracks. The third column shows the return of the underlying, and the fourth column is the NAV of the ETP calculated as # of shares multiplied by X_t + Cash (last column), all divided by the number of outstanding shares in the ETP (seventh column). The fifth column shows the return of the ETP, and the sixth contains the leverage through time, calculated as return of the ETP divided by the return of the underlying. Column six is the asset under management (AUM) of the ETP, calculated as outstanding shares in the ETP multiplied by the NAV. Column seven is the number of shares that the ETP holds in the underlying at the start of the day. Column eight is the number of shares that the ETP buys or sells at the end of the trading day.

Time	X_t	r_t^X	NAV_t	r_t^{ETP}	Leverage_t	ETP shares	AUM	# shares	Δ shares	Cash
0	400	-	100	-	-	100,000	$ 10,000,000	-25,000	-	$ 20,000,000
1	420	5%	95	-5%	-1.0	100,000	$ 9,500,000	-25,000	-	$ 20,000,000
2	428	2%	92.9	-2.2%	-1.1	100,000	$ 9,290,000	-25,000	-	$ 20,000,000
3	386	-10%	104	12%	-1.2	100,000	$ 10,361,000	-25,000	-	$ 20,000,000
4	424	10%	94	-9%	-0.9	100,000	$ 9,397,100	-25,000	-	$ 20,000,000
5	450	6%	88	-7%	-1.1	100,000	$ 8,760,926	-25,000	-	$ 20,000,000

Table X: Performance of inverse ETP that rebalances

Table X shows the development of the leverage ratio through time for an inverse ETP that rebalances the number of shares it holds in the underlying. The second column shows the value development of the underlying that the ETP tracks. The third column shows the return of the underlying, and the fourth column is the NAV of the ETP calculated as # of shares multiplied by X_t + Cash (last column), all divided by the number of outstanding shares in the ETP (seventh column). The fifth column shows the return of the ETP, and the sixth contains the leverage through time, calculated as return of the ETP divided by the return of the underlying. Column six is the asset under management (AUM) of the ETP, calculated as outstanding shares in the ETP multiplied by the NAV. Column seven is the number of shares that the ETP holds in the underlying at the start of the day. Column eight is the number of shares that the ETP buys or sells at the end of the trading day.

Time	X_t	r_t^X	NAV_t	r_t^{ETP}	Leverage_t	ETP shares	AUM	# shares	Δ shares	Cash
0	400	-	100	-	-	100,000	$ 10,000,000	-25,000	-	$ 20,000,000
1	420	5%	95	-5%	-1.0	100,000	$ 9,500,000	-25,000	2,381	$ 18,999,980
2	428	2%	93	-2%	-1.0	100,000	$ 9,310,000	-22,619	887	$ 18,619,989
3	386	-10%	102	10%	-1.0	100,000	$ 10,240,99	-21,732	-4,829	$ 20,481,585
4	424	10%	92	-10%	-1.0	100,000	$ 9,15,913	-26,561	4,829	$ 18,433,802
5	450	6%	87	-6%	-1.0	100,000	$ 8,663,900	-21,732	2,460	$ 17,327,877

C. VIX complex model

III.A. State space representation

The observation vector, $\mathbf{y}_t$, is now expanded with the variables, VIX_t and Demand_t. The observation equation is then given by:

$$\begin{pmatrix} \text{VIX}_t \\ y_t(\tau_1) \\ \vdots \\ y_t(\tau_N) \\ \text{Demand}_t \end{pmatrix} = \begin{pmatrix} 1 & 0 & 0 & 0 & 0 \\ 0 & 1 & \frac{1-e^{-\lambda\tau_1}}{\lambda\tau_1} & \frac{1-e^{-\lambda\tau_1}}{\lambda\tau_1} - e^{-\lambda\tau_1} & 0 \\ \vdots & \vdots & \vdots & \vdots & \vdots \\ 0 & 1 & \frac{1-e^{-\lambda\tau_N}}{\lambda\tau_N} & \frac{1-e^{-\lambda\tau_N}}{\lambda\tau_N} - e^{-\lambda\tau_N} & 0 \\ 0 & 0 & 0 & 0 & 1 \end{pmatrix} \begin{pmatrix} \text{VIX}_t \\ \text{Level}_t \\ \text{Slope}_t \\ \text{Curvature}_t \\ \text{Demand}_t \end{pmatrix} + \begin{pmatrix} 0 \\ \varepsilon_{1t} \\ \vdots \\ \varepsilon_{Nt} \\ 0 \end{pmatrix}, \tag{14}$$

with the state equation given by:

$$\begin{pmatrix} \text{VIX}_{t+1} \\ \text{Level}_{t+1} \\ \text{Slope}_{t+1} \\ \text{Curvature}_{t+1} \\ \text{Demand}_{t+1} \end{pmatrix} = \underset{5\times5}{(\mathbf{I}} - \underset{5\times5}{\boldsymbol{\Phi}}) \underset{5\times1}{\boldsymbol{\mu}} + \underset{5\times5}{\boldsymbol{\Phi}} \begin{pmatrix} \text{VIX}_t \\ \text{Level}_t \\ \text{Slope}_t \\ \text{Curvature}_t \\ \text{Demand}_t \end{pmatrix} + \underset{5\times1}{\boldsymbol{\eta}_t} \tag{15}$$

III.B. Filtered term structure factors of VIX complex model

Figure X: Latent factors

Figure X shows the time series of the filtered latent term structure factors from the VIX complex model, together with the empirical proxies. Correlations are; 0.85 for Level and VX8, -0.96 for Slope and VX8 minus VX1, and 0.94 for Curvature and 2×VX3-(VX1+VX8).

(a) Level

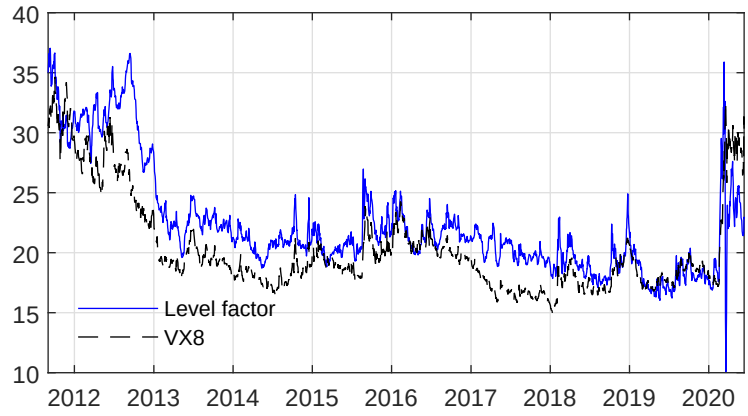

(b) Slope

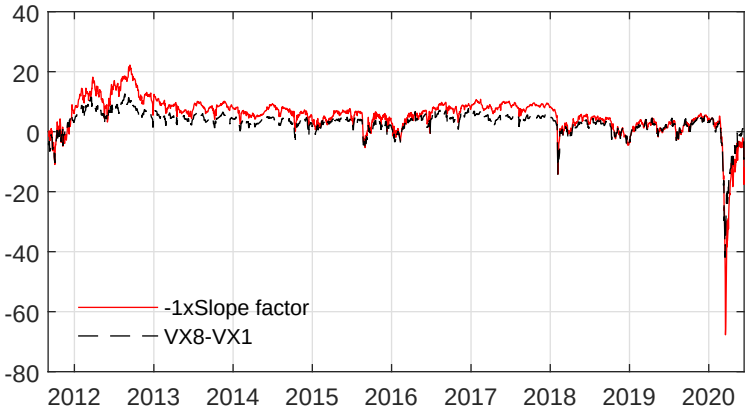

(c) Curvature